Mobile Doppler Radar Observations of an Intense Long-Lake-Axis-Parallel Lake-effect Snow band on 10-12 December 2013 During the Ontario Winter Lake-effect Systems Project

DUSTIN CONRAD, NICHOLAS ZELASKO, JEFFREY FRAME, AND JAKE MUHOLLAND

Department of Atmospheric Sciences, University of Illinois at Urbana-Champaign, Urbana, IL

1. Introduction

This study examines a long-lake-axis-parallel lake-effect snow band over Lake Ontario that occurred on 10-12 December 2013 during the Ontario Winter Lake-effect Systems (OWLeS) Project. Three Doppler on Wheels (DOW) radars, the University of Wyoming King Air instrumented aircraft, the University of Alabama-Huntsville Mobile Integrated Profiling System (MIPS), mobile rawinsonde teams, and multiple ground-based instrumented mesonets sampled this band. A map of the deployment is shown in Fig. 1.

The lake-effect snow band formed on 10 Dec over the eastern portion of Lake Ontario and persisted through the early morning hours of 12 Dec. Data collection began at 2200 UTC 10 Dec with dual-Doppler data beginning at 0027 UTC 11 Dec. Data collection ceased at 2300 UTC on 11 Dec.

The close proximity of the mobile radars to the band allows for high-resolution analyses of wind shifts and misovortices within the band. These data allow for a better understanding of the structure of these lake-effect snow bands (Steiger et al. 2013). Herein, we document two different times, one in which displays a prominent wind shift and another that depicts multiple vortices located in the band. We first discuss our methods used in the analysis of data, followed by a synoptic overview. Afterward, we examine our results from the obtained radar data and end with a presentation of our findings and plans for our future work.

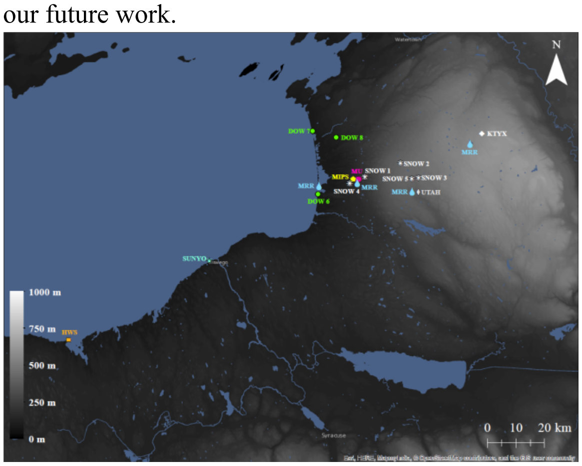

Fig 1: Location of selected ground-based OWLeS assets and the KTYX WSR-88D radar at 0120 UTC 11 December. Grayscale shading indicates elevation above mean sea level (ASL; m). Oswego, NY, is labeled as "SUNYO".

2. Data and Methodology

The DOW radars are mobile X-band (3-cm) wavelength radars with dual-polarization capabilities. The beam width is 0.93º (Wurman et al. 1997). Both DOW6 and DOW7 deployed at 2300 UTC on 10 Dec (Fig. 1) and remained in place until 0000 UTC on 12 Dec.

Data were edited using Solo3 software. If the normalized coherent power (NCP) fell below 0.3, the data were determined to be of poor quality and were removed. Areas of ground and sea clutter were manually determined from the reflectivity, radial velocity, and correlation coefficient (RHOHV) fields and were also removed.

Data were mapped to a regular Cartesian grid using a two-pass Barnes analysis (Barnes 1964). For all analyses, the horizontal grid spacing is 400 m and the vertical grid spacing is 100 m. The Barnes smoothing parameter in the horizontal directions is 1.66 km^2 and 0.059 km^2 in the vertical direction. The multiplier, gamma, for the second pass is 0.3.

3. Synoptic and Thermodynamic Environment

Between 0000 UTC and 2200 UTC on 11 December, two 500 mb shortwave troughs passed over Lake Ontario and influenced the thermodynamic environment and boundary layer depth. Figure 2a depicts 500 mb heights and absolute vorticity at 0100 UTC. At this time, Lake Ontario is east of the shortwave trough in a region of differential positive vorticity advection (DPVA), leading to ascent and midlevel cooling. A sounding from the SUNY-Oswego WRF valid at 0100 UTC for Oswego, NY, shows a deep and moist boundary layer, characterized by steep lapse rates, extending to approximately 650 mb. KTYX WSR-88D reflectivity depicts a solid, linear, snow band at 0102 UTC (Fig. 2a).

Figure 2b illustrates 500 mb heights and absolute vorticity at 1200 UTC. Lake Ontario is west of the first shortwave trough in a region of

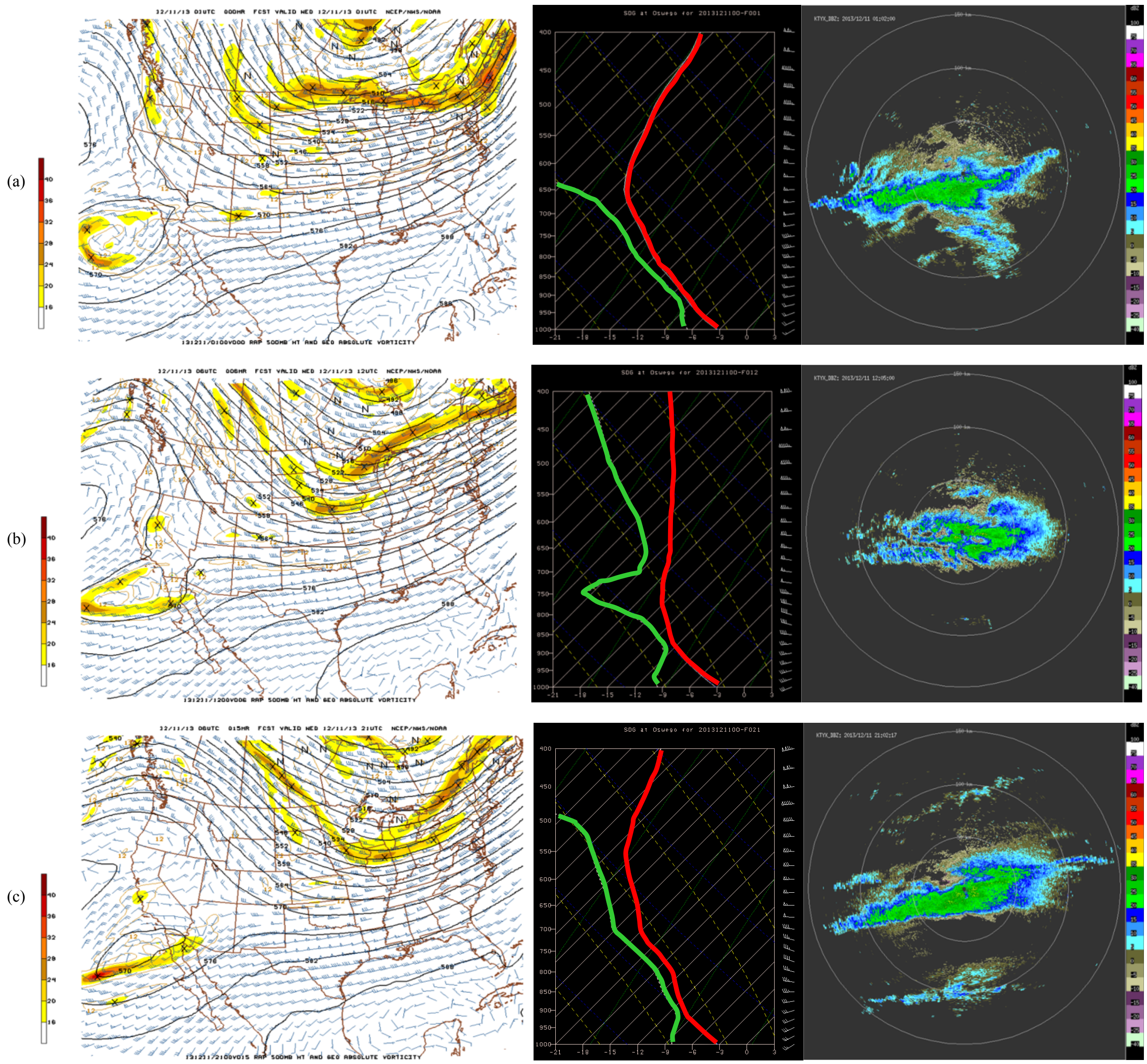

Fig 2 (a-c): 500 mb winds, heights (contoured) and vorticity (shaded); soundings from SUNY Oswego WRF, and KTYX reflectivity displayed for (a) 0100 UTC, (b) 1200 UTC, and (c) 2100 UTC. Note how that in areas of DPVA, lake-effect band is coherent and intense with strong lapse rates and a high inversion height (a & c). In areas of DNVA, lake-effect band is broken and cellular with weaker lapse rates and a lower inversion height (b). This is due to mid-level cooling/heating associated with the presence or absence of shortwave troughs.

differential negative vorticity advection (DNVA), leading to descent and midlevel warming. A sounding valid at 1200 UTC from the SUNY-Oswego WRF for Oswego, NY, indicates warming owing to subsidence in the 900-700 mb layer. A reflectivity image from KTYX WSR-88D at 1205 UTC indicates cellular, broken convection within the snow band.

Figure 2c shows 500 mb heights and absolute vorticity at 2100 UTC as a second shortwave trough approached from the west. Lake Ontario is east of the shortwave trough in a region of differential positive vorticity advection (DPVA), leading to ascent and midlevel cooling. A sounding valid at 2100 UTC from the SUNY-Oswego WRF for Oswego, NY, reveals a deep boundary layer similar to 0100 UTC, owing to midlevel cooling since 1200 UTC. KTYX WSR-88D reflectivity at 2102 UTC depicts a solid, linear band of convection.

Throughout this lake-effect event, the air-lake temperature difference was much greater than the 13ºC threshold necessary for lake-effect convection. Looking at the soundings from the SUNY-Oswego WRF at 0100 and 2100 UTC, 850 mb temperatures were approximately -15°C. Lake Ontario lake temperatures were as warm as 3-4°C, meaning air-lake temperature differences were as

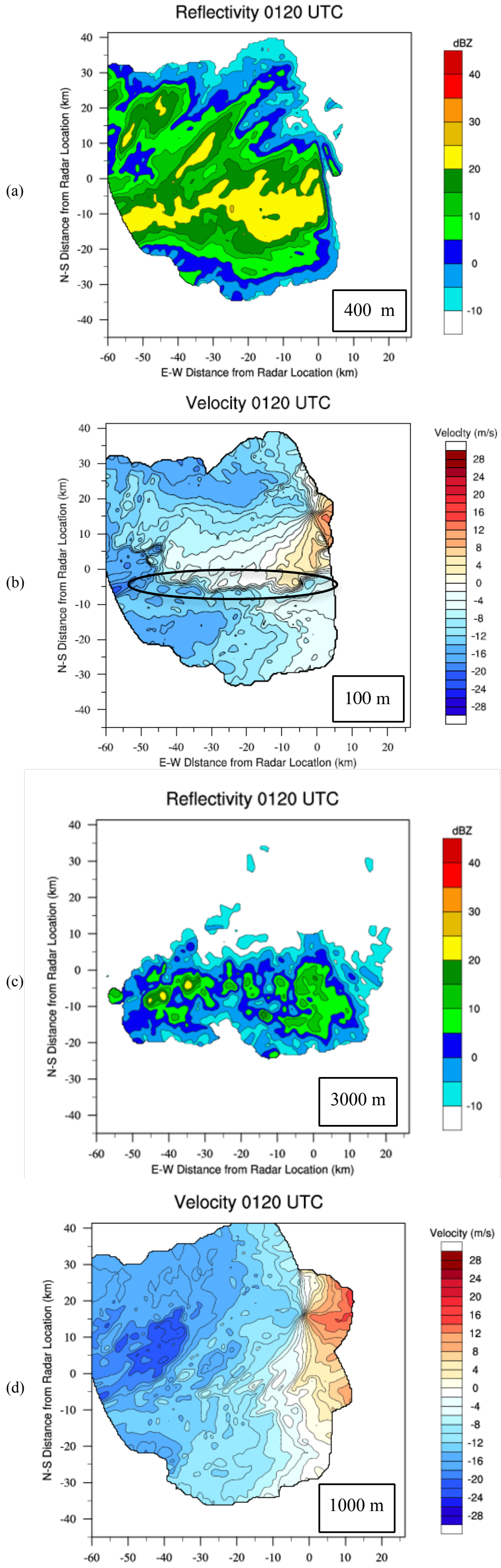

large as 18-19°C.

Another important factor that affected intensity of the snow band is wind shear. The soundings from the SUNY-Oswego WRF strong unidirectional (westerly) winds from the surface through the troposphere. Wind speeds ranged from 15-50 knots which are favorable for lake-effect convection.

4. Radar Objective Analyses

At 0120 UTC on 11 Dec, a prominent wind shift with embedded vortices was located within the snow band. Figure 3a displays objectively-analyzed radar reflectivity factor from DOW7 at 400 m above ground level (AGL). Figure 3c illustrates intense precipitation cores which extend above the top of the objective analysis domain at 3000 m.

Figure 3b shows objectively-analyzed radial velocity from DOW7 at 100 m AGL. A sharp wind shift is circled in black on this image. Within this wind shift, there are several small embedded vortices, likely owing to horizontal shear instability. The wind shift extended to just below 1000 m AGL (Fig. 3d). Winds north of the boundary were approximately northwesterly, while winds south of the boundary were approximately southwesterly, implying a secondary circulation within the band. The wind shift then propagated south, out of the band, implying other synoptic or mesoscale processes may have led to this convergence zone.

From 0930 UTC to 0947 UTC on 11 Dec, multiple vortices and intense precipitation cores were located within the snow band. The time 0937 UTC was chosen in order to include all vortices within range of DOW6 and DOW7. Figure 4a displays reflectivity at 100 m AGL, depicting intense precipitation cores located within the snow band. These cores extend up to 2000 m as shown in Fig. 4c, but barely reach the top of the objective analyses domain of 2500 m (not shown). Upper-level convergence and divergence associated with the updrafts and downdrafts within these cores can be seen in Fig. 4d, which displays radial velocity at 2000 m AGL.

Figure 4b depicts velocity at 100 m AGL, which allows for vortices located within the snow band to be seen. The strongest vortex is circled in black with weaker vortices circled in red. The strongest vortex extends to 600 m AGL, while the two weaker vortices only extend to 300-400 m AGL. The radial velocity differential across the strongest vortex is 10 m s^{-1} while only 6 m s^{-1} for the weaker vortices. This leads us to believe that these vortices are likely not caused by horizontal shear instability,

Fig 3 (a-d): Objectively-analyzed (a) radar reflectivity (dBZ) at 400 m AGL, (b) radial velocity (m/s) at 100 m AGL, (c), radar reflectivity at 3000 m AGL, and (d) radial velocity at 1000 m AGL at 0120 UTC from the DOW7 radar. Wind shift is circled in black in Fig. 3b.

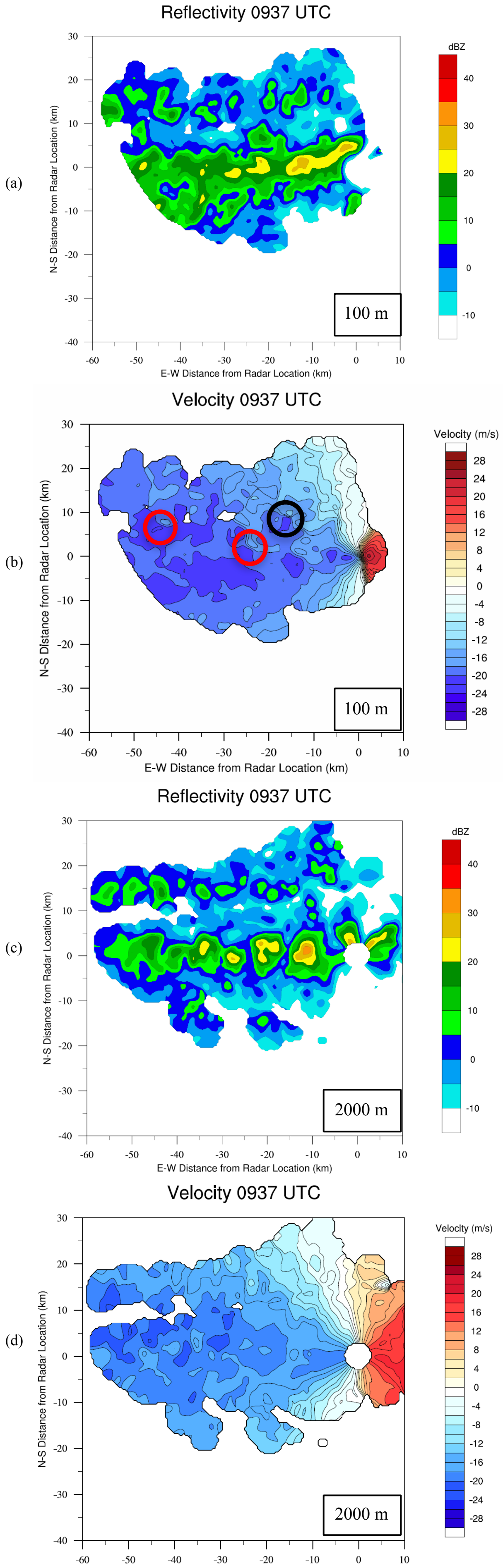

due to the lack of a prominent wind shift. Further analysis is needed in order to determine the formation mechanism of these vortices.

5. Conclusions

Differential positive vorticity advection owing to 500-mb shortwave troughs led to synoptic-scale ascent, which leads to cooling above 800 mb, a higher equilibrium level, and a more favorable thermodynamic environment for lake-effect systems. The band exhibited a more solid structure when the thermodynamic environment was more favorable (0100 and 2100 UTC), but was composed of broken cellular convection when the environment was less favorable (1200 UTC), outside of regions of orographic enhancement.

Objectively-analyzed Doppler radar data at 0120 UTC reveals a solid band with echo tops above 3000 m AGL. Also at this time, a wind shift was observed within the southern portion of the band, with vortices located along it, consistent with vortex formation owing to horizontal shear instability (Steiger et al. 2013). The wind shift extended from the surface to just below 1000 m AGL. This convergence line moved southward and cleared the southern edge of the band just after 0200 UTC.

Objectively-analyzed Doppler radar data at 0937 UTC illustrate a narrower band with the most intense cores reaching 2500 m. Single-Doppler radial velocity data depict a few vortices within the band near the northern edge of heaviest precipitation. These vortices were not located along a wind shift and are 400-600 m in depth.

6. Future Work

We plan to perform dual-Doppler wind syntheses at these and other times in order to gain a broader picture of the dynamics and kinematics within this lake-effect snow band. It is our hope that this will allows us to gain a better understanding of how these wind shifts and vortices form and whether they influence areas of more intense precipitation.

Additionally, we will investigate the thermodynamic characteristics on both sides of the southward-propagating wind shift around 0130 UTC. This will be achieved by incorporating data from soundings taken on both sides of the snow band in addition to in-situ data collected from mobile mesonet vehicles and weather pods that were deployed during this time period.

Fig 4 (a-d): Objectively-analyzed (a) radar reflectivity (dBZ) at 100 m AGL, (b) radial velocity (m/s) at 100 m AGL, (c), radar reflectivity at 2000 m AGL, and (d) radial velocity at 2000 m AGL at 0937 UTC from the DOW6 radar. Vortices circled in (b) in red have a Δv of about 6 m s^{-1} while the ones circled in black have a Δv of about 10 m s^{-1}.

Finally, we would like to examine vertically-pointing radar data from the Wyoming Cloud Radar and the UAH MIPS as well as in situ microphysical data.

Acknowledgments: We thank Prof. Bob Rauber and Joe Finlon for their assistance with radar data editing and analysis along with Christopher Johnston of UIUC for plotting the deployment map. We are grateful to all of the OWLeS volunteers who assisted with the data collection. Support from NSF Grant No. AGS 12-59257 is also acknowledged.

REFERENCES

Barnes, S. L., 1964: A technique for maximizing details in numerical weather map analysis. *J. Appl. Meteor.*, **3**, 396-409.

Steiger, S., and Coauthors, 2013: Circulations, bounded weak echo regions, and horizontal vortices observed within long-lake-axis-parallel-lake-effect storms by the Doppler on Wheels. *Mon. Wea. Rev.,* **141**, 2821-2840.

Wurman, J. M., J. M. Straka, E. N. Rasmussen, M. Randall, and A. Zahrai, 1997: Design and deployment of a portable, pencil-beam, pulsed, 3-cm Doppler radar. *J. Atmos. Oceanic Technol.*, **14**, 1502-1512.